Preprints of the 19th World Congress
The International Federation of Automatic Control
Cape Town, South Africa. August 24-29, 2014

Energy Management of Through-The-Road Parallel Hybrid Vehicles

C. Pisanti*, G.Rizzo*, V.Marano*

**Dept. of Industrial Engineering, University of Salerno, 84084 Fisciano (SA), Italy*
e-mail: cpisanti – grizzo – vmarano @ unisa.it).

Abstract: The paper presents a study on optimal energy management of through-the-road parallel hybrid vehicles, obtainable by suitably upgrading existing conventional cars. The main features and potential benefits associated to such a mild, after-market hybridization are firstly discussed, before introducing main methodological aspects, both in terms of mathematical modeling approach and benchmarks for real-time implementable control strategies. Then, a dynamic programming optimization procedure was set-up, thus allowing performing an exhaustive scenario analysis. The outcomes of such an analysis allow evaluating the fuel saving margins, within which it is possible to fall depending on the selected through-the-road vehicle architecture. Particularly, it is possible to quantify the fuel saving potential of the specific hybrid vehicle topology here examined, on one hand, and, on the other, to establish the reference benchmark, addressed by dynamic-programming derived optimality level, to which to refer when developing real-time energy management policies.

1. INTRODUCTION

In the last decade, Hybrid Electric Vehicles (HEVs) have been emerging as a feasible solution to the worldwide increasing consumption of petroleum fuels and, in turn, to the unbearable impact of carbon dioxide emissions of passenger cars fleets. However, the market share of hybrid and electric vehicles is still inadequate to produce a significant impact on a global basis. According to the blue-map scenario traced by the International Energy Agency (IEA, 2011) for the timeframe 2010-2050, the percentage of Plug-in Electric Vehicles (PEVs) sales will be still negligible before 2020, with values ranging from 1.25 (2015) to 7.5 (2020) %. Indeed, the current economic crisis could potentially negatively affect such forecasts. Moreover, in the short-term scenario a non-uniform increase in PEVs sales is expected, thus leaving room for adopting differentiated strategies worldwide to reduce green-house-gas emissions impact of passenger car fleets.

Another limiting factor to personal mobility electrification is represented by existing electric infrastructures: an uncontrolled and fast diffusion of plug-in electric vehicles could significantly impair residential distribution transformers life (Gong et al., 2012).

The reconversion of the actual vehicle fleet to hybrid is therefore gaining interest, as a short-term solution. Given the complexity of the interactions between existing conventional powertrain and hybridization options, the most convenient (in terms of trade off between cost, ease of installation and performance) and promising one consists of electrifying rear wheels in a front-wheel drive car, with after-market kits (i.e. Poulsen Hybrid, HySolarKit). This architecture is classified as a 'Through-the-Road' (TTR) Parallel HEV: the two powertrains are not directly connected to each other, as the parallel configuration is implemented through the road-tire force interaction. Some detailed studies on these vehicles have been recently published, focusing on drivability (Galvagno et al., 2013) and on control strategies for torque vectoring (Kaiser et al., 2011). In this paper, attention is focused on energy management strategies: in particular, the differences with respect to both conventional vehicles and ideally hybridized powertrains (assuming that electric motor speed is not constrained by vehicle speed, and that, for a given electric power, motor speed corresponding to the maximum electric efficiency could be adopted) will be highlighted, and the benchmarks defining the potential benefits achievable in terms of fuel saving will be analyzed, for different options and configurations.

2. TTR PARALLEL HEV

The structure of a TTR HEV includes an internal combustion engine mounted on the front axle and an electric motor that powers the rear one. Being the parallel configuration implemented through the interaction between road and tire, both axles will move at the same speed. The heat engine provides power to the front wheels, while the electric motors drive the rear wheels, or absorb power from them during the regenerative braking. In Fig. 1 the energetic flow of a TTR vehicle is represented.

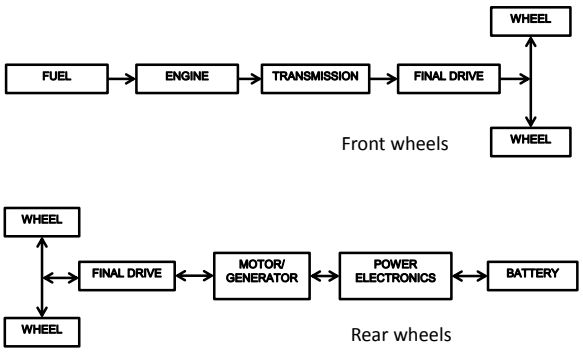

Fig. 1. Energetic flow of a TTR vehicle.

It is reasonable to expect that the benefits in terms of fuel savings would be lower respect of a native hybrid vehicle, for two main reasons:

- due to the coupling of front and rear axles, in a TTR HEV the speed of the electric motor is proportional to the speed of the vehicle; instead, in a native HEV the motor speed is not constrained by vehicle speed, and therefore it could operate near to the conditions of maximum efficiency;
- in a native HEV, part of the reduction in fuel consumption is due to engine downsizing, while these effects would be absent in a TTR HEV; however, this consideration may be misleading, since a considerable performance upgrade with respect to the starting conventional vehicle could result, depending on hybridization ratio.

The very first ancestor of a TTR HEV can be considered the Lohner-Porsche Mixte, built in 1901 by Ferdinand Porsche (http://press.porsche.com/news/release.php?id=642).

Some recent models or prototypes of TTR HEV are presented in the following:

1) ***Landi Renzo.*** This solution is still in a testing phase: the basic concept involves the installation of the electric motors inside the rims of the non-tractive wheels and a battery pack is positioned in the trunk, within the spare-wheel compartment. The hybridization kit is composed by two electric motors of 20 kW.
2) ***Poulsen Hybrid.*** In the aftermarket solution proposed by Poulsen Hybrid, the electric motors are applied directly on the original wheels via adjustable plates. A prototype has been developed through the application of Poulsen kit on Honda Civic (http://www.poulsenhybrid.com), with main specifications listed in next table:

Table 1. Technical specifications of Poulsen kit.

In - wheel motors	Brushless
	Dimensions: diameter 35.56 cm x width 7.62 cm
	Weight: 17.236kg (one wheel)
	Power: 10kW
Adjustable plates	Dimensions: diameter 100 mm or 108 mm or 114.3 mm
Controllers	96 VDC (volt direct current) max 150 A or 250 A (for each motor)
Braking system	Regenerative system
Battery	Lithium Capacity: 4.3 kWh Duration: 1000 - 2000 cycles Charger: 96V/10 A Weight: 95.25 kg
Un-sprung weight	17 kg on rear wheels

3) ***HySolarKit.*** In this project, developed at the University of Salerno, a kit for solar hybridization of front-driven cars has been developed and installed on a FIAT Punto Diesel 1.3 l (G. Rizzo et al., 2013a, www.hysolarkit.it). The conversion is obtained by installing flexible solar cells on vehicle hood and roof, an additional battery and two electrically driven in-wheel motors on rear axis. Wheel control is achieved via a VMU using data from OBD port. Data of main components are presented in Table 2.

Table 2. Technical specifications of HSK.

Nominal ICE power [kW]	75
Fuel type	Diesel
Drag coefficient [/]	0.325
Frontal area [m^2]	2.05
Rolling radius [m]	0.295
Rolling resistance coefficient [/]	0.02
Base vehicle mass [kg]	980 kg
PV installed power [kW]	0.280 kW
PV mass [kg]	4.7 kg
Li-ion battery capacity [m]	4.4 kWh
Li-ion battery voltage [V]	96 V
Li-ion battery mass [kg]	45 kg
In-wheel motors power [kW]	14 kW
In-wheel motors mass [kg]	43 kg

3. ENERGY MANAGEMENT OPTIMIZATION

A relevant literature can be found in the area of HEV energy management and control, mostly aiming at determining the best torque splitting between engine and motor (Sciarretta and Guzzella, 2007). The used approaches can be generally classified as rule-based and model-based, and further categorized according to the methodologies and the mathematical techniques adopted. A schematic view is presented in Fig. 2, where box in Italics indicate predictive approaches using telemetry (T.S. Kim, 2011).

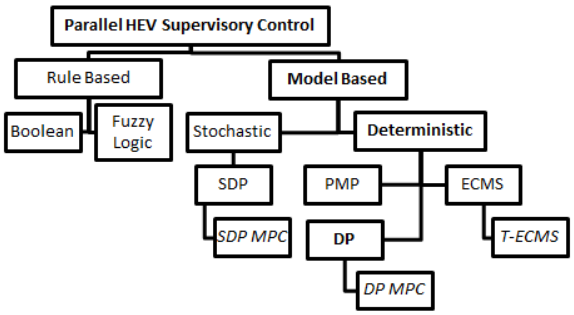

Fig. 2. Categories of control methodologies used in HEV power management (adapted from T.S.Kim, 2011)

In this paper, a Model Based Deterministic Dynamic Programming (DP) approach is used (indicated in boldface in Fig. 2). DP is a numerical algorithm based on Bellman's optimality principle (Bellman, 1957), which finds the control law providing the globally minimum value for the given objective function, while satisfying the system constraints. In this particular application, the DP is designed to find the minimum fuel consumption for a given driving cycle, while satisfying constraints on battery SOC. DP algorithms works backward starting from the final time and going back until initial time. It is therefore a non-causal method used for off-line optimization, requiring a previous knowledge of the

driving cycle (Guzzella and Sciarretta, 2009). The algorithm requires a static, discrete time model of the system. The advantage of DP, as compared to other optimization techniques (Marano et al., 2009), is to be very efficient, not to be influenced by linear or nonlinear nature of the problem and especially to always guarantee that the solution found represents the global optimum (neglecting discretization errors). On the other hand, the computational complexity of DP algorithms is exponential in the number of states and inputs. The optimization of the proposed TTR HEV is based on the DP algorithm presented in Sundstrom and Guzzella, 2009. Due to the above-mentioned features, DP-based assessment of any kind of energy management policy for hybrid vehicles is considered as the most reliable approach. Moreover, the authors themselves proved how the combined use of DP and power predictor models allow extending DP applicability from offline to online HEV control tasks (Arsie et al., 2005).

3.1. Application of DP to TTR HEV

The energy consumption of the TTR HEV vehicle is computed using a quasi-static discrete-time model. The battery state-of-charge (SOC) is assumed as the state variable. A backward longitudinal dynamic vehicle model is used, including air drag, rolling friction and inertial forces, to compute vehicle torque starting from an assigned driving cycle (Rajamani, 2012). Weight and inertia increases due to battery and wheel motors are included in the model (Sorrentino et al., 2013).

One of the most important design variables in a HEV is the hybridization factor (HF), defined as the fraction of the maximum power provided by the EM over the sum of maximum power of EM and ICE (C. Hoder and J. Gover, 2006; Lukic and Emadi, 2004):

$$HF=\frac{P_{EM,max}}{P_{EM,max}+P_{ICE,max}} \quad (1)$$

The optimal range of HF values for different HEVs has been analyzed in literature (O. Sundstrom et al., 2008). When hybridizing a conventional vehicle, the addition of excessive electric power may result in vehicle unbalance and should be avoided. Thus, a HF near 20% has been chosen for this study.

The ratio between the electric power and the total power to the vehicle P_{Veh}, defined as Power Split, is the main decision variable in HEV energy management:

$$PS(t)=\frac{P_{EM}(t)}{P_{Veh}(t)}=\frac{P_{EM}(t)}{P_{EM}(t)+P_{ICE}(t)+P_{Brake}(t)} \quad (2)$$

where P_{Brake} (≤ 0) is the power absorbed by mechanical brakes. The correspondences between PS values and TTR HEV operating modes are listed in .

Table 3. Power Split values.

PS=1	Electric mode
0<PS<1 $P_{EM}>0$	Hybrid mode (traction)
0<PS<1 $P_{EM}<0$	Regenerative braking
PS=0	Thermal mode
PS<0	Hybrid recharging mode

The model can be summarized by following equations:

$$x_{k+1}=f(x_k,u_k,v_k,a_k,i_k)+x_k \qquad k=0\ldots N \quad (3)$$

where the index k represents time, and N the number of time steps.

State and control variable can be expressed formally respectively by **Errore. L'origine riferimento non è stata trovata.-Errore. L'origine riferimento non è stata trovata.**):

$$x_k=SOC(k) \quad (4)$$

$$u_k=PS(k) \quad (5)$$

where v_k is the vehicle speed, a_k is the vehicle acceleration, and i_k is the active gear index. It can be noticed that, for each time step, v_k, a_k and i_k are known in advance, since DP requires a previous knowledge of the driving cycle. State transition can be then expressed by:

$$x_{k+1}=f(x_k,u_k)+x_k \quad k=0\ldots N \quad (6)$$

The cost function to be minimized can be expressed by next equation:

$$C=\sum_{k=0}^{N-1}\Delta m_f(u_k,k)\cdot T_s \quad (7)$$

where the terms under summation is the mass of fuel consumed at time k. The following equations describe the boundary conditions for the state variable:

$$x_0=SOC_0 \quad (8)$$

$$x_N=SOC_N\pm\varepsilon \quad (9)$$

$$x_k\in[SOC_{min}\ SOC_{max}] \quad (10)$$

The following values (see Table 4) have been used in the paper, unless otherwise specified:

Table 4. Time step, SOC boundary conditions for DP.

Time step	$T_s=1$[s]
SOC starting and final values	$SOC_0=SOC_N=0.7$
SOC limit values	$SOC_{min}=0.6$, $SOC_{max}=0.8$
Final SOC tolerance	$\varepsilon=0.001$

The optimization problem has been solved in Matlab through the algorithm proposed by Sundstrom and Guzzella (2009).

The analyses presented in the next sections were accomplished by means of a longitudinal vehicle model developed under the following hypotheses: *i)* the drag force is

considered acting on vehicle center of gravity; *ii)* vehicle inertia accounts for both vehicle mass and rotational inertia of ICE, EM/EG and wheels; *iii)* the effects of elasticity in the mechanical transmission are neglected. Furthermore, ICE fuel consumption is computed through a normalized map, starting from experimental data.

4. DATA OF THE OPTIMIZATION ANALYSIS

The data used for vehicle, battery and electric motor are shown in Table 5. The battery is modeled adopting an equivalent circuit model, consisting of a voltage source and a resistance in series. Internal and external resistance dependence on state of charge variation is taken into account via look-up tables derived from the literature (Guzzella and Sciarretta, 2012). Two in-wheel motors are considered: their efficiency map is shown in Fig. 3. The wheel motors used at University of Salerno for a prototype of a solar hybridization kit have been considered (Rizzo et al., 2013 b). It is worth noting that their efficiency and power density are lower than those characterizing the best off-the-shelf products available today.

Three standard driving cycles have been selected for this analysis: i) New European Driving Cycle (NEDC), ii) Federal Urban Driving Schedule (FUDS) and iii) Federal Highway Driving Schedule (FHDS).

Table 5. Data used for the analysis.

5.	Variable	Data
Conventional vehicle	Original vehicle weight [kg]	1030
	Frontal area [m^2]	2.04
	Aerodynamic drag coefficient [/]	0.325
	Engine power [kW]	51
	Rpm max [rpm]	5500
	Torque max [Nm]	110
	Fuel	Gasoline
	Engine	1.2 l SI
Battery	Mass [kg]	15
	Capacity [Ah]	6
	Max discharging current [A]	100
	Max charging current [A]	125
	Voltage [V]	270
Electric motor (each wheel motor)	Mass [kg]	27.2
	Power max[kW]	7
	Rpm max [rpm]	1300

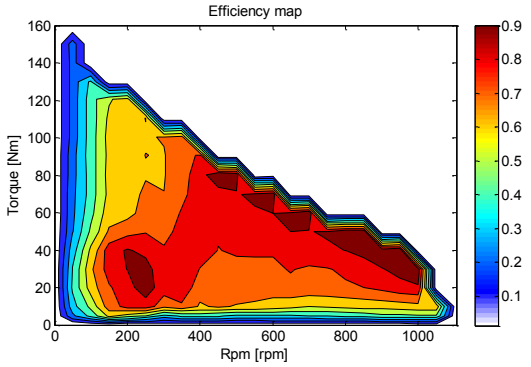

Fig. 3. Electric motor efficiency map

For the optimization analysis, different vehicle architectures have been considered:

1) **Conventional Vehicle (CV)**: this case is used as reference;
2) **Ideal Powertrain Hybridization (IPH)**: it is assumed that electric motor speed is not constrained by vehicle speed, and that, for a given electric power, motor speed corresponding to the maximum electric efficiency could be adopted; it should be noticed that in this case, unlike in a native HEV, there are not downsizing effects with respect to the conventional vehicle;
3) **TTR with drive by wire (DBW)**: TTR HEV, with no limits on PS values, as explained below;
4) **TTR**: TTR HEV with upper limits on PS (0.5/0.7).

The differences between cases 3 and 4 depend on the connection between gas pedal and engine ECU on the TTR HEV. If the gas pedal is directly connected to the original ECU (case 4), when the driver steps on the accelerator, so demanding higher vehicle power, an increase in the engine power will necessarily result. And, similarly, a reduction in engine power will be always achieved when the driver releases gas pedal. Therefore, for a given vehicle power demand, when PS increases, less power increase is demanded to the engine: gas pedal range decreases, so increasing pedal sensitivity to vehicle power (Fig. 4). If PS tends to 1 (pure electric mode), pedal range would tend to zero, and the vehicle could not be driven. Therefore, a suitable maximum value of PS has to be set in hybrid mode (G. Rizzo et al., 2013a). Of course, pure electric mode (PS=1) would be always possible when the engine is off.

Instead, if a drive by wire connection is adopted (i.e. the gas pedal is connected to a VMU that in turn drives the ECU), the increase in vehicle power could be achieved even by reducing the engine power and, in parallel, by increasing the electric motor power: therefore, there are not limitations on PS values (case 3).

Optimal fuel consumptions, computed for each case, are shown in Table 6. In all cases, charge sustaining operation is considered, with SOC values specified in Table 4.

CO_2 emissions (g/km) have been computed through (11).

$$CO_2 = \frac{100}{FE} \cdot \phi \tag{11}$$

where FE is fuel economy and the coefficient ϕ has been taken from EU Technical Guidelines (2013), as shown in Table 7.

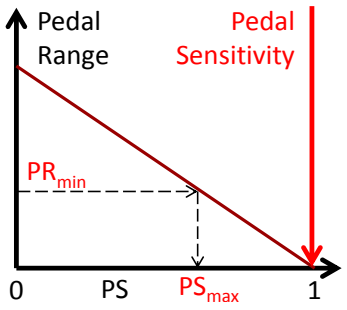

Fig. 4. Pedal range and sensitivity vs. PS (qualitative)

Table 6. Fuel economy (km/l) for different driving cycles.

Scenario	NEDC	%	FUDS	%	FHDS	%
1.CV	15.09	0	14.67	0	16.82	0
2.IPH	16.75	11	17.68	20.52	17.30	2.85
3.TTR DBW	16.13	6.89	16.61	13.22	16.93	0.65
4a.TTR PS≤0.7	15.52	2.85	16.24	10.70	16.78	-0.24
4b.TTR PS≤0.5	15.32	1.52	16.16	10.16	16.76	-0.36

Table 7. Conversion fuel consumption → CO_2 emission

Type of fuel	Conversion factor (g/ l)
Gasoline	23.3
Diesel	26.4

Main results are presented in Table 8**.** For each case, the percent reduction with respect to the conventional vehicle is also shown. It emerges that, as expected, the maximum CO_2 reduction with respect to the conventional vehicle are achieved with case 2, without constraints on motor speed and PS. The benefits gradually decrease while increasing constraints on motor speed and maximum PS values. The results also confirm that the advantages of the hybrid propulsion are maximized in urban driving, especially in cycles characterized by prevailing transient operation (FUDS), and are relatively lower, or even slightly negative in cases 4a and 4b, for highway driving (FHDS). These negative values can be explained considering that the vehicle model accounts for weight and inertia increase due to hybridization. Moreover, it has to be remarked that no downsizing effects are achieved when hybridizing an existing vehicle (but, on the other hand, vehicle performance is significantly enhanced). Maximum benefit is about 17% for IPH case over FUDS cycle, decreasing to 11.7% with TTR with DBW. The presence of further constraints on PS values (cases 4a and 4b) produces a slight reduction of hybridization benefit, to 9.70% and 9.28%, with respect to TTR with DBW.

6. OPTIMAL CONTROL LAWS ANALYSIS

In this paragraph the main control laws resulting from the optimization are shown and analyzed. For the sake of brevity, the results are referred to urban cycles (FUDS and NEDC), where major benefits are obtained (Table 6, Table 8).

In Fig. 5 the SOC values obtained with or without limitations on PS are shown. It can be observed that SOC trends are quite similar in the three cases, with also similar values of fuel consumptions (Table 6). Therefore, it emerges that PS limitations have little influence on fuel consumption in urban driving cycles.

Table 8. CO_2 emissions (g/km) and reduction (%).

Scenario	NEDC	%	FUDS	%	FHDS	%
1.CV	154.37	0	158.9	0	138.5	0
2.IPH	139.14	9.87	131.8	17.04	134.7	2.76
3.TTR DBW	144.47	6.41	140.3	11.71	137.7	0.63
4a.TTR PS≤0.7	150.18	2.71	143.5	9.70	138.8	-0.22
4b.TTR PS≤0.5	152.11	1.46	144.1	9.28	139.1	-0.38

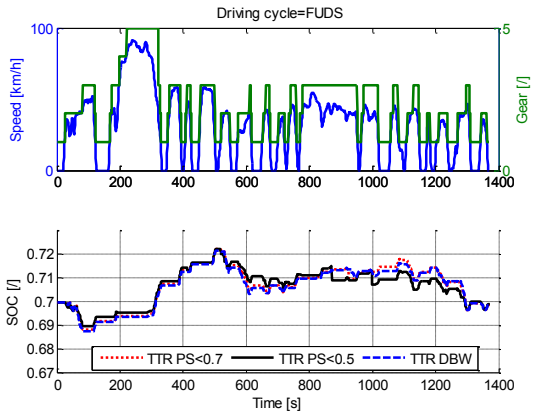

Fig. 5. SOC values for different TTR configurations.

The following plot (Fig. 6) shows the contribution of rear wheels over total vehicle torque. The points on the bisector refer to PS=1. They only occur during regenerative braking, since during traction maximum PS is 0.7. Both for positive and negative values, wheel motor torque tends to saturate to its maximum values for large positive or negative values of vehicle torque. It can be also observed that, during traction, null PS values (i.e. thermal mode) are often selected, while recharging mode (negative wheel motor torque with positive vehicle torque) is almost never proposed. The distribution of PS in case of negative vehicle torque is shown in Fig. 7. Similar graphs have been obtained for all the examined cases. The analysis of PS for NEDC driving cycle, that is a combination of a urban and an extra-urban driving cycle, is shown in Fig. 8. While in the urban fraction PS values of TTR with and without limitations almost overlap, they are quite different during the extra-urban fraction. It can be observed that during the urban fraction (T<800 s) recharging mode (PS<0) is never selected, while it is selected in a few occurrences during extra-urban driving. Moreover, when wheel motors are activated, PS tends to saturate to its maximum value (1 for TTR with DBW and 0.7 in the other case). It must be noticed that values PS>0.7 with the red line correspond to regenerative braking.

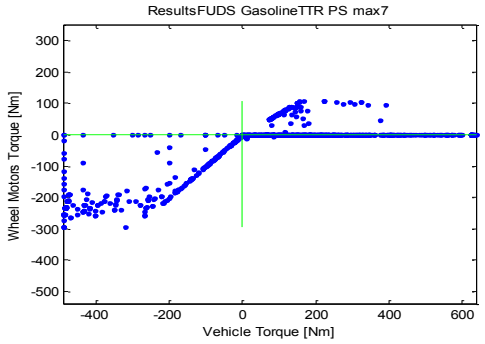

Fig. 6. Wheel Motors Torque vs. Vehicle Torque – TTR PS<0.7 - FUDS cycle.

The case of TTR with the constraint PS<0.7 on FUDS cycle is shown in Fig. 9, where power to front wheels, rear wheels and mechanical brakes is presented at the top. Also in this case, it can be observed that PS tends to saturate to its maximum value 0.7, even if intermediate values (0<PS<0.7) are also selected. Recharging mode (PS<0) is rarely proposed. Fig. 10 shows that SOC values differ from the case

of Ideal HEV before T=900 s, even if trends are similar, while they are almost overlapping for T>900 s.

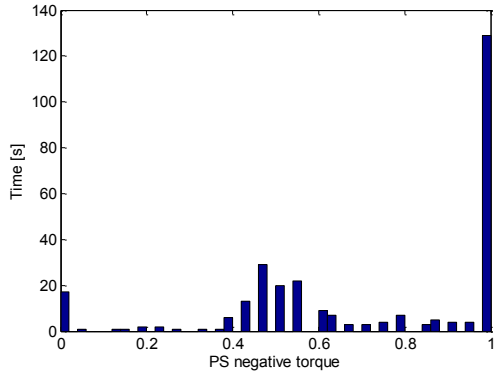

Fig. 7. Distribution of PS during deceleration mode (TTR PS<0.7 - FUDS cycle).

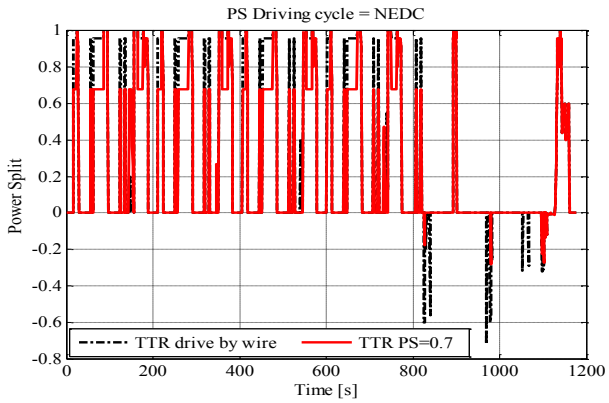

Fig. 8. PS values (NEDC cycle) for different architectures of TTR, with or without limitation on PS.

The fact that in most cases the Wheel Motor torque tends to saturate to its maximum value (Fig. 6) suggest that a possible simple implementable control strategy could be realized by adopting the maximum allowable Power Split (i.e. 0.7) in traction mode, when compatible with actual SOC values, and the unit value of PS during braking mode. A detailed analysis of the results to test this strategy and to develop more articulate management strategies is in progress.

6.1. Effects of electric motor efficiency

All the results previously presented refer to the efficiency map shown in Fig. 3. In order to evaluate the effects of the motor efficiency, a parametric analysis has been performed.

The percent gain in fuel consumption with respect to the results presented in Table 6 can be analyzed through improved efficiency maps: these efficiency values have been computed considering the following equation:

$$\eta_{new}(\text{rpm, torque}) = \frac{\eta(\text{rpm, torque})^{z1}}{\eta_{max}} \cdot (1+z_2) \qquad (12)$$

where η_{new}(rpm, torque) is the new wheel motor efficiency map, developed by applying (12) to the original map η(rpm, torque), and η_{max} is the maximum original map efficiency value (see Fig. 3). The results of the scenario analysis, carried-out by updating the original map by varying the parameters z_1 and z_2 (12), highlight how more performing electric motors would result in increasing fuel economy, as high as 18%, as compared to the performance achievable with the considered map. It is worth mentioning here that the contour plot shown in Fig. 11 was obtained by excluding all those couples (z_1, z_2), whose application via (12) would have led to non-meaningful wheel motor efficiency map.

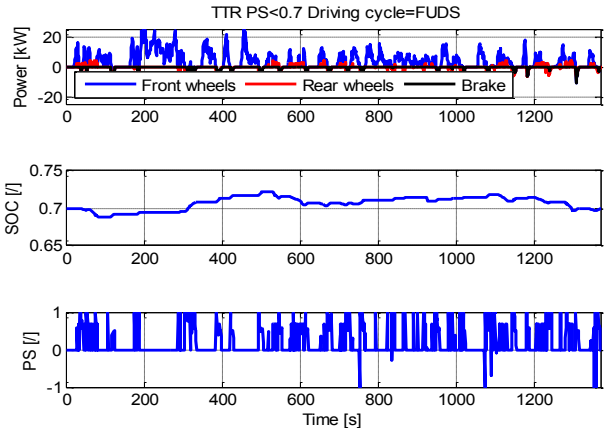

Fig. 9. Main variables for TTR with Ps<0.7 and FUDS driving cycle.

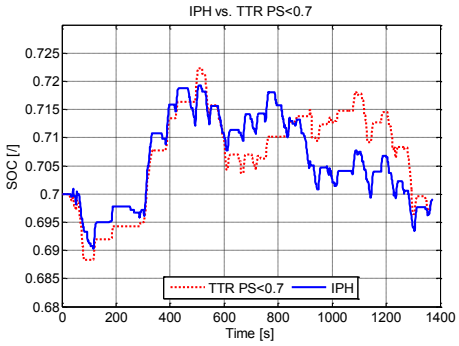

Fig. 10. SOC values of a TTR HEV vehicle vs. HEV, for a driving cycle FUDS.

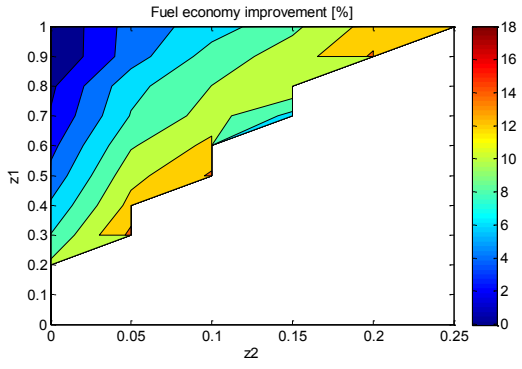

Fig. 11. Fuel economy improvement with respect to the base case. The vehicle architecture and driving cycle here considered are TTR-DBW and FUDS, respectively.

7. CONCLUSIONS

HEV TTR architecture is gaining interest, due to the possibility to hybridize conventional cars by integration of wheel motors on not driving wheels (usually the rear ones). The benefits in terms of fuel consumption and emissions are

still interesting, but lower with respect to a native HEV, due both to the speed constraints for wheel motors and on the absence of downsizing effects in the ICE. On the other hand, significant improvement in performance and acceleration with respect to the base vehicle would result.

In the paper, the optimal energy management for different configurations has been studied via Dynamic Programming. The effects of constraints on wheel motors speed due to the TTR architecture and of possible limitations on Power Split ratio due to the presence or absence of Drive by Wire (DBW) have been analyzed and quantified. Even without DBW, the benefits in urban driving (FUDS) are over 9%, while they are absent in highway (FHDS), as expected. Recharging mode is rarely selected in the examined cases, mostly due to the relatively low efficiency assumed for wheel motors. The results improve significantly when adopting more performing electric components.

Further work is in progress to extend this analysis to vehicle powered by Diesel engines and to develop and validate on-board Rule-Based implementable strategies. Moreover, the impact of switching from charge sustaining to charge-depleting battery management will be investigated. Thus, it will be possible to assess the additional benefits achievable by including a photovoltaic roof in the hybridizing kit, as well as of enabling the plug-in mode.

8. REFERENCES

Arsie, I., M. Graziosi, C. Pianese, G. Rizzo, M. Sorrentino (2005). Control Strategy Optimization for Hybrid Electric Vehicles via Provisional Load Estimate. In: *Review Of Automotive Engineering*, Vol. 26, pp. 341-348.

Bellman, R. E.,(1957). *Dynamic programming*. Princeton, University Press, Princeton - N.J.

European Commission (February 2013). *Technical Guidelines for the preparation of applications for the approval of innovative technologies pursuant to Regulation (EC)*. No 443/2009 of The European Parliament and of the Council.

Galvagno, E., D. Morina, A. Sarniotti, M. Velardocchia (2013). Drivability analysis of through the road parallel hybrid. *MECCANICA*, 48 n. 2, 351-366.

Gong, Q., S. Midlam-Mohler, V. Marano, G. Rizzoni, (2012). Study of PEV Charging on Residential Distribution Transformer Life. In: *IEEE Transactions on Smart Grid,* 3: 1. 404-412.

Guzzella, L., and A. Sciarretta (2013). Vehicle Propulsion Systems. *Third Edition, Springer.*

Hoder, C., and J. Gover (2006). Optimizing the hybridization factor for a parallel hybrid electric small car. In: *Proceedings of IEEE Vehicle Power and Propulsion Conference*, pp. 1-5.

HySolarKit, available at http://www.hysolarkit.it

IEA (2011). Technology Roadmap: Electric and plug-in hybrid electric vehicles. Available at http://www.iea.org/publications/ freepublications/publication/EV_PHEV_Roadmap.pdf.

Kaiser G., F. Holzmann, B. Chretien, M. Korte, H. Werner (2011). Torque Vectoring with a feedback and feed forward controller applied to a TTR HEV. In: *Proceeding of IEEE Intelligent Vehicles Symposium,* pp. 448-453.

Kim, T. S., (2011). Optimal Control of a Parallel Hybrid Electric Vehicle with Traffic Preview. *PhD Thesis,* University of Melbourne.

Lukic and Emadi (2004). Effects of Drivetrain Hybridization on Fuel Economy and Dynamic Performance of Parallel Hybrid Electric Vehicles. In: *IEEEE Transactions on Vehicular Technology*, Vol. 53, pp. 385-389.

Marano, V., Medina H., Sorrentino M., Rizzo G.. (2013a). A Model to Assess the Benefits of an After-Market Hybridization Kit based on Realistic Driving Habits and Charging Infrastructure. In: *SAE Int. J. Alt. Power*. Vol. 2(3), doi:10.4271/2013-24-0086.

Marano V., Muratori M., Rizzo G., Rizzoni G. (2013b). Sustainable Mobility: from Fossil Fuels to Renewable Energy, Opportunities and Challenges for the Automotive Industry. In: *7th IFAC Symposium on Advances in Automotive Control, National Olympics Memorial Youth Center,* Tokyo.

Marano V., Tulpule P., Stockar S., Onori S., Rizzoni G. (2009). Comparative study of different control strategies for plug-in hybrid electric vehicles. In: *SAE Technical Paper,* 2009-24-0071, doi: 10.4271/2009-24-0071.

Poulsen Hybrid, available at http://www.poulsenhybrid.com/

Rajamani, R., (2012). *Vehicle Dynamics and Control.* Springer.

Rizzo, G., C. Pisanti, M. D'Agostino, M. Naddeo (2013a). Driver Intention Analysis for a Through-the-Road Solar Hybridized Car. In: *SAE Technical Paper,* 2013-24-0079, doi:10.4271/2013-24-0079.

Rizzo, G., V. Marano, C. Pisanti, M. D'Agostino, M. Naddeo, M. Sorrentino, I. Arsie (2013b). A Prototype Mild-Solar-Hybridization Kit: Design and Challenges. IN: *Proceedings of 68th Conference of the Italian Thermal Machines Engineering Association, ATI2013.*

Sciarretta, A., L. Guzzella (2007). Control of Hybrid Electric Vehicles. In: *IEEE Control Systems Magazine*, Vol. 27-2, pp. 60-70.

Sorrentino, M., C. Pianese, M. Maiorino (2013). An integrated mathematical tool aimed at developing highly performing and cost-effective fuel cell hybrid vehicles. In: *Journal of Power Sources*, Vol. 221, pp. 308–317.

Sundstrom, O. and L. Guzzella (2009). A Generic Dynamic Programming Matlab Function. In: *Proceedings of the 18th IEEE International Conference on Control Applications,* pp. 1625-1630, Saint Petersburg, Russia.

Sundstrom, O., L. Guzzella and P. Soltic (2008). Optimal hybridization in two parallel hybrid electric vehicles using dynamic programming. In: *Proceedings of the 17th IFAC World Congress,* Seoul, Korea.